

Original Paper

Systematic Evaluation of Compressive Toughness of Confined Concretes Based on Constitutive Model

Shigemitsu HATANAKA, Yasuo TANIGAWA*, and Hiroki HATTORI**
(Department of Architecture)

(Received September 17, 1991)

Firstly, discussion is carried out on the magnitude of lateral confining pressure required to keep concrete ductile under compression for various strength level. Next, the reinforcing efficiency of various types of lateral reinforcement is evaluated. The compressive deformation behavior of confined concretes can be predicted only by putting the presently introduced reinforcing efficiency and the lateral pressure calculated from the volume of reinforcement into a constitutive model proposed earlier.

Key Words: confined concrete, constitutive relation, compressive toughness, stress-strain relation, ductility, lateral pressure

1. Introduction

It has been pointed out that the mechanism of the toughness improvement of confined concrete and steel fiber reinforced concrete under compression is mainly due to the lateral confining effect of lateral bars and steel fibers caused by the Poisson's effect of concrete after failure [1-6]. This effect can be easily related to the behavior of plain concrete under multiaxial stress states. Thus, it is possible to discuss systematically the toughness improvement by various kinds of lateral confinement, based on the triaxial compression test data.

The authors, therefore, developed a triaxial testing method in which a high rigidity compression testing machine and a new type of lateral loading device are combined, which enables the examination of the plastic deformation behavior of axially loaded concrete subjected to low lateral confining stresses

* Department of Architecture, Faculty of Engineering, Nagoya University

** Tokyu Corporation

[7]; then proposed an evaluation method for the effect of various types of lateral confinements on the compressive toughness of concrete, based on the constitutive (stress-strain) model for concrete under triaxial compression [8].

The main purposes of this study is to discuss how much lateral confining pressure is required to keep concrete ductile under compression, and to evaluate the compressive toughness of circular and rectangular confined concretes by means of "equivalent lateral pressure" applying the proposed stress-strain model.

2. Stress-strain model used

2.1 Longitudinal stress-strain relation for triaxial compression

The authors have already proposed a numerical expression of stress (σ_1)-strain(ϵ_1) curve in the direction of the maximum principal compressive stress for plain concrete under the following condition.

Shape of specimen: $H/D=1$ (H:height, D:diameter or width of section)

Stress path of lateral pressure: active loading

Ratio of two lateral stresses: $\sigma_2/\sigma_3=1$

Loading area of lateral pressure: uniformly distributed

Table 1 Formulas for σ_1 - ϵ_1 curves

Strength Failure Criterion (σ_{1f})

$$f(I_1, J_2, \cos 3\theta) = A \frac{J_2}{\sigma_c^2} + \lambda \frac{J_2}{\sigma_c} + B \frac{I_1}{\sigma_c} - 1 = 0 \quad \text{----- (1)}$$

where, I_1 : First invariant of stress tensor, J_2, J_3 : Second and third invariants of stress deviator tensor, respectively, σ_c : Uniaxial compressive strength (positive value), $\lambda = \lambda(K_1, K_2, \cos 3\theta)$, $\cos 3\theta = 1.5\sqrt{3} \cdot J_3/J_2^{3/2}$, A, B, K_1, K_2 : Empirical parameters.

Strain Failure Criterion (ϵ_{1f})

$$\epsilon_{1f}/\epsilon_c = -|I_{1f}/\sigma_c|^a \quad \text{----- (2)}$$

where, ϵ_c : Strain at uniaxial compressive strength (positive value), I_{1f} : I_1 at failure.

Relative Stress (σ_1/σ_{1f}) - Relative Strain (ϵ_1/ϵ_{1f}) Relation

$$\text{Stress ascending portion: } \frac{\sigma_1}{\sigma_{1f}} = \frac{n_a \cdot \epsilon_1 / \epsilon_{1f}}{n_a - 1 + (\epsilon_1 / \epsilon_{1f})^{n_a}} \quad \text{----- (3a)}$$

$$\text{Stress descending portion: } \frac{\sigma_1}{\sigma_{1f}} = \frac{1}{n_d} + \frac{(n_d - 1) \cdot X}{n_d - 1 + X^{n_d}} \quad \text{----- (3b)}$$

$$n_d = \bar{\alpha} n_{d1} \quad \text{----- (3c)}$$

where, $\sigma_{1f}, \epsilon_{1f}$: Stress and strain at failure in the direction of maximum principal compressive stress, $X = (\epsilon_1 / \epsilon_{1f})^m$, $n_a = E_1 / \{E_1 - (\sigma_{1f} / \epsilon_{1f})\}$, $n_d = \bar{\alpha} n_{d1}$, $n_{d1}: n_d$ for uniaxial compressive stress state, E_1 : Initial modulus of elasticity, $m, \bar{\alpha}$: Empirical constants.

Here, active loading means the stress path that the lateral stresses are applied to a specimen before axial loading. Table 1 and Figs. 1(a) and (b) show the outline of the proposed model and examples of a set of $\sigma_1 - \epsilon_1$ curves, respectively.

2.2 Lateral pressure required for sufficient compressive ductility

Figures 2(a) and (b) show lateral confining pressure (σ_L) required to maintain stress as large as uniaxial compressive strength even after the peak point (hereinafter, non-softening type), which is indicated in Figs.1(a) and (b). The value of σ_L required for the $\sigma_1 - \epsilon_1$ curve of non-softening type (${}_{R}\sigma_L$) increases with the increase in the compressive strength (σ_c) of concrete. The approximate value of ${}_{R}\sigma_L$ is $\sigma_c/20$ for specimens of H/D=1 and $\sigma_c/10$ for the specimens of H/D=2, where the value of ${}_{R}\sigma_L$ becomes large as strain ϵ_1 increases.

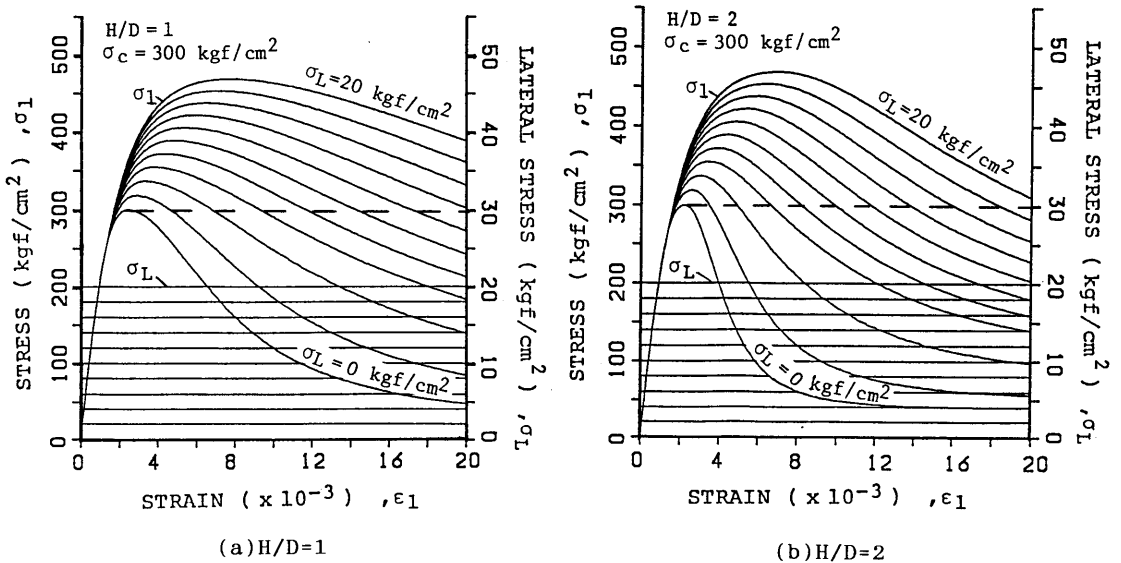


Fig.1 Examples of a set of $\sigma_1 - \epsilon_1$ curves by proposed model

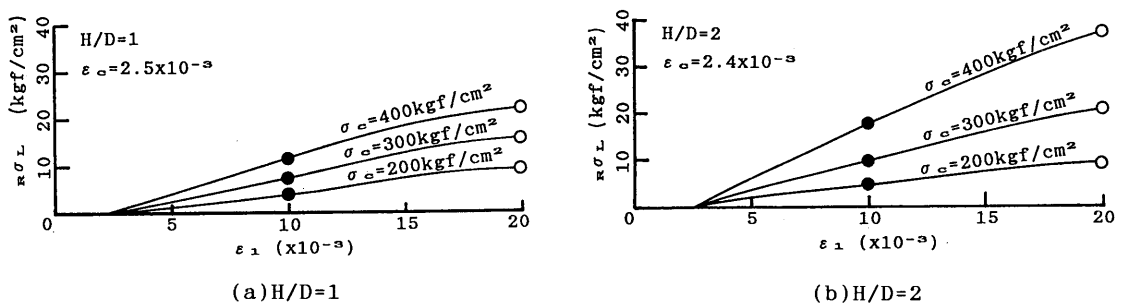


Fig.2 Required lateral confining pressure

3. Reinforcing efficiency of circular hoops (Exp.-I)

3.1 Experimental procedures

The outline of Exp.-I is shown in Table 2. All the specimens used were cylindrical and 10 cm in diameter. Table 3 shows the arrangement of circular hoops and calculated lateral pressure ($H\sigma_{LY}$) at the yielding of the hoops. Here, the calculated lateral pressure means the pressure applied to a specimen on the condition that the hoop is arranged uniformly in the longitudinal direction of a specimen. Ordinary Portland cement, river sand (maximum size: 5 mm), river gravel (size range: 5 - 15 mm), steel fiber (size: 0.5x0.5x30 mm, tensile strength: 7000 kgf/cm²), and steel ring (inner diameter: 10 cm) were prepared for the fabrication of concrete.

All the specimens were loaded in the longitudinal (first) direction under the constant strain rate of about 2×10^{-3} /min. by using a high rigidity compression testing machine. The friction at the specimen-loading platen interfaces was reduced by placing friction reducing pads. The pad consists of two polypropylene sheets with silicon grease between them. A couple of differential transformers were set between loading platens to measure the overall strains and also a couple of W.S.G.'s for concrete strain. The strain of steel rings were measured by a couple of W.S.G.'s.

Table 2 Outline of Exp.-I

W/C	V _f (%)	H/D	Hoop
0.55	0	1	A~G
		2	A,C,E,G
	0.75	1	A~F
	1.5		A,C,E
0.45	0		A,C,E
0.70			

[Notes] W/C:Water-cement ratio, V_f:Volume fraction of steel fiber, H/D:Height/width of specimen.

Table 3 Arrangement of circular hoops and calculated lateral pressure

Notation of specimen	Hoop		P _s (%)	H ^σ LY (kgf/cm ²)
	Arrange* (H/D = 1)	Pitch (cm)		
A		∞	0	0
B		10	0.08	2.3
C**		10	0.16	4.6
D		5	0.16	4.6
E**		5	0.32	9.2
F		2.5	0.32	9.2
G**		2.5	0.64	18.4

[Notes] p_s:Sectional area of hoop/Sectional area of specimen, H^σLY=p_s·σ_{sy}/100, σ_{sy}:Yield stress of hoop(=2870 kgf/cm²), *:Section of hoops:-----1.6x2.5 mm, ——1.6x5.0 mm, **: W.S.G.'s are glued to hoops.

3.2 Test results and discussion

(1) Stress-strain and equivalent lateral pressure curves

Figure 3 shows examples of measured $\sigma_1 - \epsilon_1$ curves and equivalent lateral pressure ($\bar{\sigma}_L$) corresponding to each $\sigma_1 - \epsilon_1$ curve. The equivalent lateral pressure holds almost a constant value after the peak point.

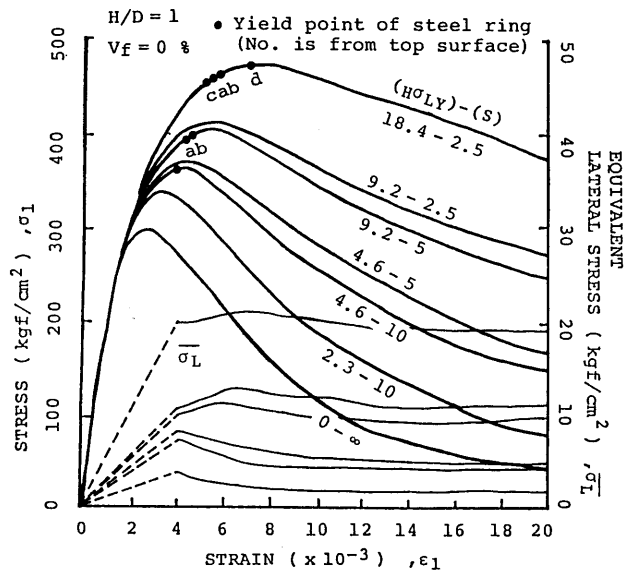


Fig.3 Measured $\sigma_1 - \epsilon_1$ curves and equivalent lateral pressure curves

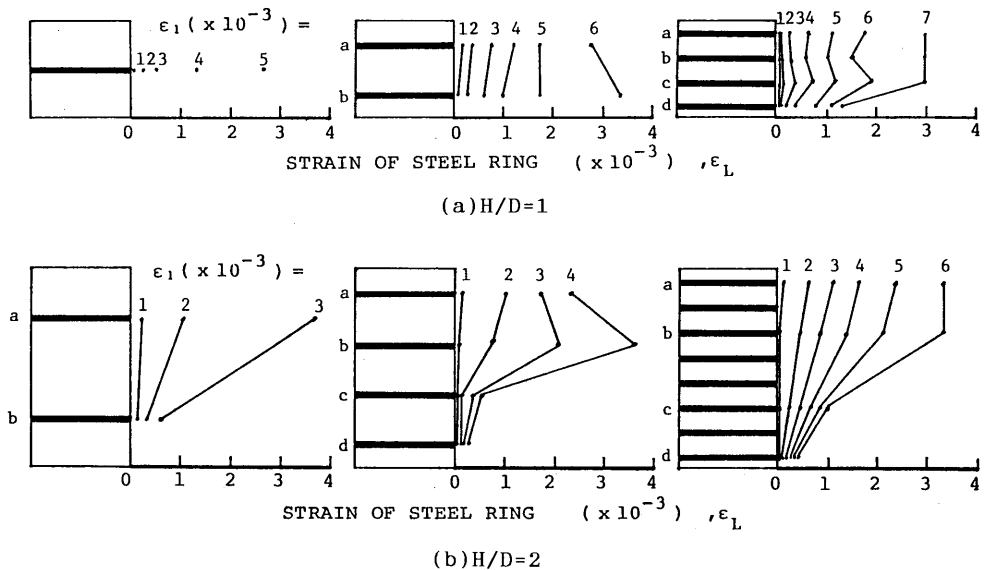


Fig.4 Variation of strain of steel rings

(2) Failure pattern of specimen and variation of strain of steel rings

Figures 4(a) and (b) show the variation of strain of steel rings (circular hoops) for the specimen of H/D=1 and 2, respectively. The strain of steel rings or lateral strain of concrete increases almost uniformly in any height over a specimen for H/D=1, while in case of H/D=2 the lateral strain of concrete in the top half in casting increases more rapidly than that in the bottom half.

Figure 5 shows the calculated lateral pressure (${}_H\sigma_L$) corresponding to the strain of steel rings in the specimens of H/D=2 shown in Fig.4(b). According to Figs.3 through 5, all the rings yield (yield strain $\epsilon_L = 1.37 \times 10^{-3}$) at around the peak point of $\sigma_1 - \epsilon_1$ curve for the specimens of H/D=1; while the strain of the ring in the bottom of specimens gradually decreases at around $\epsilon_1 = 10 \times 10^{-3}$, and the ring does not yield even in the ultimate state for the specimens of H/D=2. Therefore, in case of H/D=2, the lateral confining capacity of the steel rings is not fully utilized.

(3) Reinforcing efficiency of circular hoops

To discuss the reinforcing efficiency of circular hoops, the equivalent lateral pressure (σ_L^*) in the stress descending range was averaged. The reinforcing efficiency (R) is defined as follows:

$$R = \sigma_L^* / {}_H\sigma_{LY} \tag{1}$$

where, σ_L^* : averaged equivalent lateral pressure

${}_H\sigma_{LY}$: calculated lateral pressure at the yielding of hoops

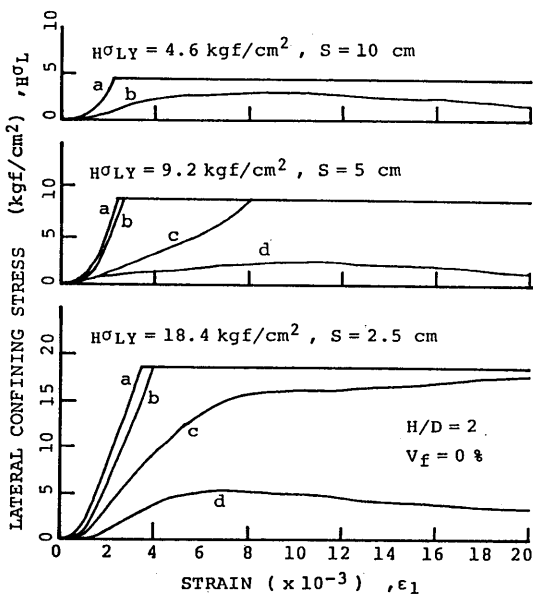


Fig.5 Variation of calculated lateral pressure by hoops (H/D=2)

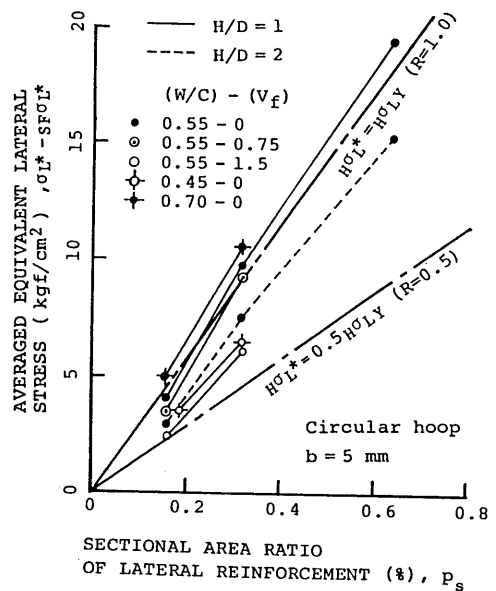


Fig.6 Averaged equivalent lateral pressure by circular hoops

Figure 6 shows the comparison between the calculated lateral pressure by yielded hoops ($h\sigma_{LY}$) and the averaged equivalent lateral pressure by hoops ($h\sigma_L^*$). Here, for fiber reinforced concrete, the value of $h\sigma_L^*$ is calculated by reducing the averaged equivalent lateral pressure due to steel fiber ($s_f\sigma_L^*$) from σ_L^* ; that is $h\sigma_L^* = \sigma_L^* - s_f\sigma_L^*$, where value of $s_f\sigma_L^*$ is regarded based on the test data as 5.5 kgf/cm² for $V_f=0.75\%$ and 10 kgf/cm² for $V_f=1.5\%$. In most cases, the lateral reinforcing capacity of hoops is sufficiently utilized, the reinforcing efficiency (R) being almost unity. For $H/D=2$ or $W/C=0.45$ ($F_c=360$ kgf/cm²), however, the value of R is about 0.7 to 0.8.

4.Reinforcing efficiency of rectangular hoops and ties (Exp.-II)

4.1 Experimental procedures

The outline of Exp.-II is shown in Table 4. Rectangular hoops, ties with various shapes, or their combinations shown in Table 5 were used as a lateral reinforcement. The table also shows lateral pressure ($s\sigma_L$, nominal value for non-circular reinforcement) at the yielding of steel bars calculated on the condition that all the lateral bars uniformly surround a cylindrical specimen. Water/ cement ratio was kept to 0.55 and all the specimens were prisms having 10x10 cm section. The thickness of cover concrete was zero.

4.2 Test results and discussion

Figure 7 shows the examples of $\sigma_1-\epsilon_1$ curves and equivalent lateral pressure ($\bar{\sigma}_L$) corresponding to each $\sigma_1-\epsilon_1$ curve. The reinforcing efficiency

Table 4 Outline of Exp.-II

V _f (%)	H/D	Cast*	Lateral bar	
			S(cm)	Shape
0	1	V	5	b~g
	1	V	2.5	a
1.5	2	H	5	
			10	
			∞	

[Notes] V_f:Volume fraction of steel fiber, H/D:Height/width of specimen, Cast*: Casting direction,,S:Pitch.

[Notes] *:Yield stress of steel bar (σ_{sy}) is 2970 kgf/cm² in general, **:With steel bar of $\sigma_{sy}=6700$ kgf/cm²
 P_V:Volume fraction of lateral bar,
 $s\sigma_L = P_V/2 \cdot \sigma_{sy}/100$.

Table 5 Arrangement of rectangular hoops and ties

Notation of specimen	Lateral bar		P _V (%)	s σ_L^* (kgf/cm ²)
	Shape	Pitch (cm)		
a		2.5	1.12	16.8
		5	0.56	8.4 (18.8)**
		10	0.28	4.2
b		5	1.00	15.0
c			0.84	12.6
d			0.70	10.5
e			0.98	14.7
f			0.96	14.4
g			0.96	14.4

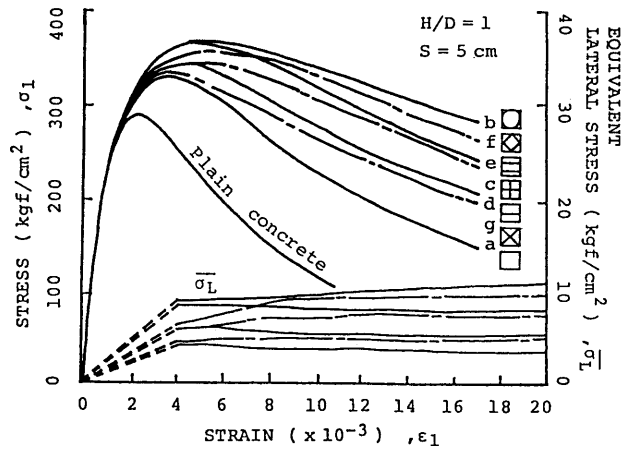
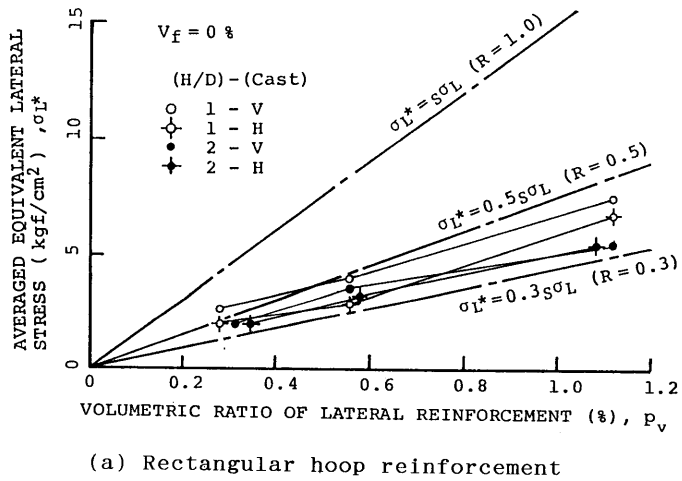
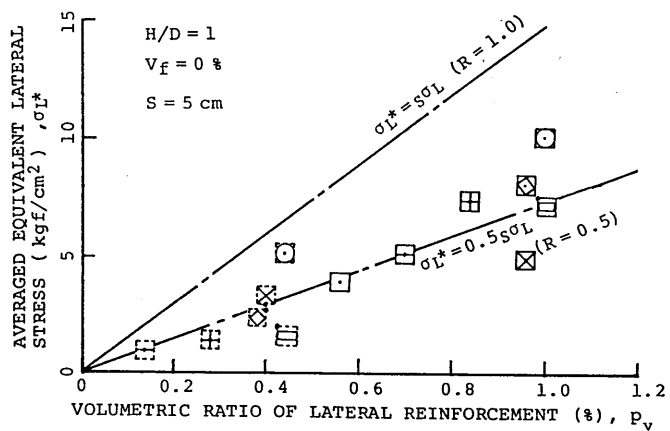


Fig.7 Measured $\sigma_1 - \epsilon_1$ curves and equivalent lateral pressure curves



(a) Rectangular hoop reinforcement



(b) Combination of rectangular hoop and tie reinforcement

Fig.8 Averaged equivalent lateral pressure by rectangular reinforcements

of rectangular hoops, ties, and the combination of them is discussed by applying Eq.(1) in the same manner as circular hoops. Figures 8(a) and (b) show the averaged equivalent lateral pressure (σ_L^*).

According to Fig.8(a), the reinforcing efficiency ($R=\sigma_L^*/s\sigma_L$) of the rectangular hoops is 0.3 to 0.5 regardless of the volumetric ratio of the reinforcement, which is about a half value for the circular hoops. The reinforcing efficiency of the rectangular hoops for $H/D=2$ is smaller than that for $H/D=1$, as well as the circular hoops.

Figure 8(b) shows the reinforcing efficiency of the rectangular hoops, ties, and the combination of them. Mostly, the reinforcing efficiency is 0.5 regardless of the type of lateral reinforcement. Generally, the higher reinforcing efficiency is attained for the higher uniformity of lateral reinforcement in a lateral section.

5. Conclusions

1) In order to keep concrete non-softening type or to maintain the stress as large as compressive strength σ_c , following magnitude of lateral confining pressure ($r\sigma_L$) is required: $r\sigma_L \geq \sigma_c/20$ for $H/D=1$, and $r\sigma_L \geq \sigma_c/10$ for $H/D=2$; where H/D is the height/width of specimen.

2) Lateral reinforcement arranged around the non-damaged zone of a specimen can not sufficiently show its confining capacity. Therefore, it is quite important to take into account the localization of damage for the discussion of compressive toughness of concrete.

3) Following values were obtained as the reinforcing efficiency (R) of lateral reinforcement: $R=0.7$ to 1.0 for circular hoops, $R=0.3$ to 0.6 for rectangular hoops and the combination of rectangular hoops and ties.

References

- 1) Shah, S.P. and Rangan, B.V.: Fiber Reinforced Concrete Properties, Jour. of ACI, 68, No.2, 126-135 (1971.2).
- 2) Bazant, Z.P. and Bhat, P.D.: Endochronic Theory of Inelasticity and Failure of Concrete, Jour. of EM Div., Proc. of ASCE, 102, No.EM4, 701-722 (1976.8).
- 3) Ahmad, S.H.: Properties of Confined Concrete Subjected to Static and Dynamic Loads, Ph.D. Thesis, Univ. of Illinois at Chicago Circle, 375pp. (1981).
- 4) Ahmad, S.H. and Shah, S.P.: Stress-Strain Curves of Concrete Confined by Spiral Reinforcement, Jour. of ACI, 79, No.6, 484-490 (1982.6).
- 5) Shimizu, M: Analytical Study on Confining Effect of Lateral Reinforcing Bar on RC Column (in Japanese), Proc of Annual Meeting of A.I.J., 1251-1252 (1982.10).

6)Tanigawa,Y., Yamada,K., Hatanaka,S., and Mori,H.: A Simple Constitutive Model of Steel Fire Reinforced Concrete, The Int'l Jour, of Cement Composites, 5, No.2, 87-96 (1983.5).

7)Kosaka.Y., Tanigawa,Y., and Hatanaka,S.: Lateral Confining Stresses Due to Steel Fibers in Concrete under Compression, The Int'l Jour. of Cement Composites, 7, No.2, 81-92 (1985.5).

8)Hatanaka,S., Kosaka,Y., and Tanigawa,Y.: Plastic Deformational Behavior of Axially Loaded Concrete under Low Lateral Pressure, Jour. of Struct. and Const. Eng. (Trans. of Architectural Institute of Japan), 377, 27-40 (1987.7).